Implicit Versus Explicit Convective Heating in Numerical Weather Prediction Models

JOHN MOLINARI AND MICHAEL DUDEK

Department of Atmospheric Science, State University of New York at Albany, Albany, NY 12222

(Manuscript received 31 May 1985, in final form 28 March 1986)

ABSTRACT

The ability of several explicit formulations of convective heating to predict the precipitation associated with a mesoscale convective complex was compared to that of a cumulus parameterization on a ½ deg latitude-longitude mesh. In the explicit approaches, prediction equations were present for both water vapor and cloud water, or vapor alone. The simplest explicit approach, for which any condensed water was assumed to fall immediately as rain, produced localized excessive rainfall. This explicit heating instability arose as a result of the requirements of saturation prior to rainfall, which delayed condensation and allowed excessive convective instability to build, and neglect of eddy fluxes, which prevented the instability from being released in a realistic manner. These results, combined with those of previous investigators, indicate that the simplest form of explicit heating is prone to instability and unsuitable for mesoscale models.

Instability problems were significantly reduced by the inclusion of the inhibiting effects of rainwater evaporation and a cloud phase with hydrostatic water loading. Nevertheless, because significant rain occurred in nature in the absence of area-averaged saturation, rainfall was unrealistically delayed when a 100 percent saturation criterion was used. Reducing the saturation criterion improved the phase error of the rainfall prediction, but sometimes reintroduced local instability.

Although only simple explicit formulations were used, inclusion of more sophisticated microphysical parameterizations from cloud models may be unrepresentative of processes in nature for meso-α scale models, for which the grid spacing exceeds 50 km. It is proposed for such models that implicit approaches offer the greatest potential for improvement. For meso-β scale models the optimum choice remains uncertain.

1. Introduction

Linear studies of the growth of disturbances in a saturated convectively unstable atmosphere (e.g., Lilly, 1960) showed that the dominant growth rate occurred at the smallest scale. In practice, this meant that uncontrolled growth would occur at the smallest resolvable scale of a numerical model if saturation were allowed to develop under convectively unstable conditions. Kasahara (1961) appeared to confirm this when his numerical simulation of a hurricane contained localized rapid growth of disturbances that obscured any larger scale feature. The concept of cumulus parameterization was designed to avoid this difficulty by postulating the *implicit* presence and properties of unresolvable subgrid-scale clouds. These implicit clouds reduce or eliminate convective instability and produce precipitation, generally in the absence of grid-scale saturation. Cumulus parameterizations vary considerably in their closure conditions, which relate the implicit clouds to the grid-scale variables. Frank (1983) provides a review of currently used approaches.

Using a hydrostatic hurricane model on a 20 km grid, Rosenthal (1978) showed that if the feedback of convection on the grid scale were incorporated, unstable small-scale growth was prevented and cumulus parameterization became unnecessary. This feedback in Rosenthal's study involved primarily rainwater evaporation, which increases low-level stability, but can also involve rainwater drag. Both of these effects oppose excessive updraft development at a single grid point. Rosenthal's approach has been termed explicit heating because, to the extent possible in a hydrostatic model, the cumulus cloud is directly simulated on the grid scale. Condensation cannot occur until saturation is reached, and the grid scale variables directly represent the properties of the "cloud." Rosenthal (1978) noted the single greatest advantage of explicit heating: it allows a broad spectrum of interactions between the convective scale (to the extent it is resolved) and larger scales. In principle, the explicit approach allows all of the closures associated with cumulus parameterization, while not restricting the interaction to any one. Because convective scale–large scale interactions may vary enormously in, for example, a forming hurricane and a frontal cyclone, this advantage of the explicit approach is potentially important in mesoscale prediction, especially during the incipient stages of convectively driven disturbances, when rotational constraints on the flow are often weak (Ooyama, 1982).

Rosenthal (1979) noted that results of hurricane simulations using cumulus parameterization were highly sensitive to arbitrarily chosen procedures. He suggested that an explicit approach, which allowed a

wider range of interaction with the larger scale without producing unstable growth once realistic inhibiting effects were added, was a better choice for models with grid spacings of 10–20 km. Ross and Orlanski (1978) used such a grid spacing to simulate moist frontogenesis with an explicit approach. Recently, several modelers have successfully adopted variations of the explicit approach on somewhat larger scales. Anthes et al. (1983) simulated explosive oceanic cyclogenesis with a 45 km grid spacing, and both Orlanski and Ross (1984) and Hsie et al. (1984) simulated frontogenesis with grid spacings of 60 and 40 km, respectively.

Despite these successes, however, some difficulties have also been reported in the use of explicit heating. Koch et al. (1985), Dare et al. (1985) and Phillips (1979) have reported localized excessive rainfall "blowups," each with meso-α scale models (grid spacing 50–250 km). Zack et al. (1985) reported unrealistic delays in the start of precipitation and a large underestimate of 6-h rainfall, followed by small-scale excess rainfall. Molinari and Corsetti (1985) reported that predicted rainfall in a mesoscale convective complex was underestimated by 96 percent over 12 h using explicit heating on a one degree latitude–longitude (~100 km) mesh, while a convective parameterization produced a reasonable forecast.

In addition to these somewhat contradictory findings, the nature of the scale dependence of the choice between implicit and explicit convective heating has not been established. The authors listed above who successfully adopted explicit formulations used grid spacings as large as 60 km, yet Fritsch and Chappell (1980) and Frank and Cohen (1985) use implicit methods on scales of 20–30 km, indicating their belief that such scales are too large to explicitly resolve cumulus effects. The issue is further complicated by the spectrum of possible explicit approaches due to variations in microphysical parameterizations.

From this brief review, it is apparent that no consensus exists on how to incorporate cumulus convection in mesoscale models. In the current paper, the choice between implicit and explicit approaches will be addressed in terms of convective heat and moisture sources and sinks. The cause and possible prevention of explicit instabilities will be described. The ability of an implicit and various explicit formulations to predict the rainfall associated with a mesoscale convective complex (MCC) on a ½° grid spacing will be investigated, and recommendations will be made as to the potential use of the two approaches in meso-α scale numerical models.

2. Implications of explicit heating

Following Molinari (1985) and analogous to Yanai et al. (1973), a *convective* apparent heat source and moisture sink can be defined as

$$Q_1' = \pi\left(\frac{\partial\bar{\theta}}{\partial t} + \bar{\mathbf{v}}\cdot\nabla\bar{\theta} + \bar{\omega}\frac{\partial\bar{\theta}}{\partial p} - g\frac{\partial F_H}{\partial p}\right) - Q_R$$

$$= L(c-e) - \pi\overline{\omega'\frac{\partial\theta'}{\partial p}} \quad (1)$$

$$Q_2' = -L\left(\frac{\partial\bar{q}}{\partial t} + \bar{\mathbf{v}}\cdot\nabla\bar{q} + \bar{\omega}\frac{\partial\bar{q}}{\partial p} - g\frac{\partial F_q}{\partial p}\right)$$

$$= L(c-e) + L\overline{\omega'\frac{\partial q'}{\partial p}} \quad (2)$$

where

$$\pi = c_p\left(\frac{p}{p_0}\right)^{R/c_p}.$$

Equations (1)–(2) group radiative heating Q_R and boundary layer fluxes F_H and F_q with the large-scale terms. Horizontal eddy fluxes are neglected and ω' is understood to be produced by convection only.

In all of the work using explicit heating described in section 1, the authors implicitly assumed that subgrid-scale vertical fluxes were zero, i.e., no parameterization of subgrid-scale eddies was present and vertical transports were produced only by the grid scale ω. From (1)–(2), it is clear that for these forms of explicit heating, $Q_1' = Q_2' = L(c - e)$ at every level, so that heating is determined directly by the local condensation rate. Thus the question of whether to use implicit or explicit heating can simply be viewed in terms of whether observations on the scale of the grid for the phenomenon being simulated have shown a significant departure of Q_1' from Q_2' (in terms of the Yanai et al., 1973, symbolism, whether or not $Q_1 - Q_R \approx Q_2$ above the boundary layer). The value of Q_1' would equal Q_2' for nonzero eddies only if the eddy temperature and moisture fluxes had an identical vertical structure; this has not been observed.

On the synoptic scale, numerous observational studies have shown that Q_1' and Q_2' differ substantially, and thus that eddy fluxes are important. On the scale of a single grid point in mesoscale models (10–75 km), however, observations of apparent heat source and moisture sink are unavailable; even in the high-resolution SESAME data, the smallest mean rawinsonde station separation is about 80 km. As a result, whether or not to parameterize cumulus convection in mesoscale models cannot be answered with current observations.

In addition to neglect of vertical eddy fluxes, explicit heating imposes an additional requirement, that saturation must be achieved before precipitation can occur. Synoptic-scale studies (e.g., Yanai et al., 1973) show that convective precipitation occurs in the absence of area-averaged saturation, but once again, much less information is available on smaller scales. This issue has been approached indirectly in the work discussed earlier (Molinari and Corsetti, 1985; hereafter

MC). When a simple form of explicit heating was used, forcing by nonconvective processes was insufficient to produce significant rainfall on a one degree latitude–longitude mesh under circumstances in nature where widespread heavy convective rain occurred. In a parallel integration with cumulus parameterization, convective rainfall initiated well before the grid saturated, subsequent enhanced vertical circulations were forced by convective heat sources and sinks, and total rain volume was predicted to within 12 percent.

Previous work suggests the following summary: For a grid spacing of 10–20 km, Rosenthal (1978) showed that, although obvious limitations are imposed by clouds 20 km on a side, the explicit approach has several advantages over the implicit approach. For grid spacing greater than or equal to 100 km, the saturation requirement imposes too serious a constraint on condensation, Q_1' differs substantially from Q_2', and a parameterized approach is required. The current paper will address the scales in between, for which the choice is much less clear cut.

3. Types of explicit heating

The term explicit heating covers a range of microphysical parameterizations in hydrostatic mesoscale numerical models (see Hsie and Anthes, 1984). In the simplest form, to be referred to as Type I (e.g., Anthes et al., 1983), any condensed water vapor is assumed to fall instantaneously as rain. No cloud stage is included, and rainwater evaporation, if present, can occur only during the time step that rain occurs.

In the second type of explicit heating, a cloud-water prediction equation is incorporated (e.g., Ross and Orlanski, 1982) of the general form

$$\frac{\partial q_{cl}}{\partial t} = -\mathbf{v}\cdot\nabla q_{cl} - \omega\frac{\partial q_{cl}}{\partial p} + c - e - r_w \tag{3}$$

where q_{cl} is cloud-water mixing ratio, c and e are rates of condensation and evaporation, and r_w is conversion of cloud to rainwater. In this form of explicit heating, condensation produces cloud water that is advected horizontally and vertically and evaporates when encountering subsaturation. The conversion of cloud to rainwater is most simply determined by the excess of cloud water over some critical value (Takeda, 1965), taken from 0.55 g kg^{-1} (Hsie and Anthes, 1984) to 1.5 g kg^{-1} (Ross and Orlanski, 1982). A simple hydrostatic "water loading" effect can be incorporated by defining a liquid water virtual temperature in the hydrostatic equation (Ross and Orlanski, 1982; Hsie and Anthes, 1984) as

$$\frac{\partial z}{\partial p} = \frac{-RT_{vl}}{pg} \tag{4}$$

where

$$T_{vl} = T_v(1 - l). \tag{5}$$

This equation represents the effects of cloud water on buoyancy; actual rain drag, of course, cannot be incorporated into a hydrostatic model. In this Type II explicit heating, rainwater, once formed, is again assumed to fall instantaneously.

Type III explicit heating incorporates a rainwater prediction equation (e.g., Hsie et al., 1984). The assumption of instantaneous rainwater fallout is replaced by an assumed terminal velocity, and such processes as accretion of cloud droplets by rain and more sophisticated evaporation of rain are incorporated. More complex microphysics, for instance prediction equations for frozen particles (Lord et al., 1984), has not been incorporated into meso-α scale models.

Regardless of the level of microphysics, all of the above approaches qualify as explicit because they have a fundamental characteristic in common: grid-scale properties and cloud properties are synonymous. Even though cumulus parameterization schemes may also contain microphysical effects (e.g., Kreitzberg and Perkey, 1976), they differ from explicit approaches in that convective effects are calculated in the absence of grid-scale saturation, and the implicit cloud properties (temperature, moisture, sometimes vertical motion) are specified in terms of, but differ from, their grid-scale counterparts. These are the fundamental properties of a cumulus parameterization. It should be noted that models containing a cumulus parameterization still make use of an explicit formulation for precipitation at convectively stable grid points.

In the current paper, only Type I and Type II explicit approaches will be tested. Potential difficulties with an extension to Type III in meso-α scale models will be discussed in section 6.

4. Model description

Except as noted below, the model equations, structure, and finite differencing follow MC. The model physics includes a bulk aerodynamic boundary layer and a diurnal cycle over land following Fritsch and Chappell (1980), modified by a simple parameterization of cloud effects, which simply reduces the amplitude of the diurnal cycle in the presence of convective rainfall or saturation at any level (see MC for details). The convection scheme in the model follows MC, except for the alterations listed below. The procedure uses the framework of Kuo (1974), Kanamitsu (1975), and Krishnamurti et al. (1976). The approach forces the sounding toward a limiting state represented by θ_c and q_c at a rate which depends upon the strength of forcing, the precipitation efficiency, and the presence of surface fluxes. The limiting state, following MC, incorporates a bulk treatment of cumulus and mesoscale downdrafts. Downdraft properties have been made more realistic than in MC by the following changes.

(i) The condition on equivalent potential temperature at cumulus downdraft top is $\theta_{ed} = \bar{\theta}_{es}$ rather than $\frac{1}{2}(\theta_{eu} + \bar{\theta}_e)$, where θ_{eu} is the updraft θ_e. One-dimensional

integrations with the new condition, which follows Johnson (1976), showed stabilization rates very close to those of the previous formulation. Nevertheless, the current form was found to more reliably produce a cumulus downdraft with enough negative buoyancy to reach the lowest levels during heavy convective rainfall.

(ii) As suggested by MC, both cumulus and mesoscale downdrafts are lagged in time, i.e., do not enter the limiting profile for 20 min (cumulus) or 2 h (mesoscale, following Zipser, 1980), after which they linearly increase in influence to their full value over one additional lag period.

(iii) Mesoscale downdraft relative humidity (r_m) has been reformulated. As in MC, the value of r_m follows Leary and Houze (1980) and the mesoscale downdraft descends from the melting level with constant θ_e. In MC, however, as the column moistened, the Leary–Houze values, which represent a fairly vigorous mesoscale downdraft, became so much drier than the environment that the downdrafts became too warm to sink even 200 mb below their top, despite the presence of a crude water loading effect. Because they had insufficient buoyancy, the mesoscale downdrafts were not incorporated into the limiting state. This was most likely to occur late in the convective life cycle, when these downdrafts should be most common. In MC, this problem was corrected by requiring $r_m > \bar{r}$, where $\bar{r}$ was the mean environmental relative humidity in the downdraft layer. An unfortunate by-product of this condition was that mesoscale downdrafts were frequently cold at all levels (see Fig. 2a of MC), whereas in nature they are often slightly warmer than their surroundings at low levels. In the current work, a more realistic r_m is defined by increasing the Leary–Houze values by 5 percent at all levels whenever the mesoscale downdrafts have insufficient buoyancy. This incrementing, which cools the downdraft due to the constant θ_e requirement, continues if necessary until the mesoscale downdraft reaches at least to 850 mb. The resultant downdrafts are closer in temperature and moisture anomaly to those observed.

Other details of the approach are described by MC.

In the explicit heating formulation, Type I and Type II approaches are tested. In the former, rainfall evaporation is computed layer by layer, starting from the top, and is allowed to moisten to 90 percent of saturation. The procedure follows the relative humidity equation approach of Kanamitsu (1975; see appendix B of MC) by evaporating all liquid water in a layer, then recondensing if necessary until $r = 90$ percent.

The Type II formulation uses Eq. (3) as a cloud-water prediction equation, with cloud water assumed to be zero initially. The critical q_{cl} value above which rain is assumed to occur is taken as 0.5 g kg^{-1}. Water loading is incorporated via Eq. (4)–(5).

One change was made in finite differencing in the model: a fourth-order Shuman "semimomentum" scheme was used for horizontal advection (Grammeltvedt, 1969). This higher order differencing produced significant improvement in phase error over the second-order approach. Other model characteristics are given by MC.

5. Results

Table 1 describes the experiments carried out in this study, all on a ½° latitude–longitude mesh, and Table 2 gives the predicted rain volume, maximum point value, and phase error of the maximum versus observations. Experiment 1 contains the parameterized heating control; the others use explicit heating, but vary in what physical effects are incorporated. Each forecast is for 12 h starting from 1200 GMT 19 July 1977.

Figure 1a, b shows predicted rainfall after 12 h using parameterized heating, and the analyzed point value amounts from Bosart and Sanders (1981; note variation in units and map scale). For verification with model runs, the maximum rainfall averaged over ½° latitude–longitude regions must be compared; this area-averaged maximum still occurs in northwest Pennsylvania, with a magnitude of approximately 6 cm. The parameterized integration overestimates the rain volume, but captures the heavy rain axis from north of Lake Erie to west central Pennsylvania, and the axis from southeastern Michigan to Pennsylvania. The predicted maximum is slightly south-southeast of that observed, but with comparable magnitude to the grid area-averaged maximum. The reason for the larger error in rain volume than for the coarser integration of MC is not clear, but overall the parameterized heating produces a reasonable rainfall prediction.

One feature of the observed precipitation field was not predicted by any of the eight experiments. Satellite pictures from Bosart and Sanders (1981) show the development of a squall line (physically separate from the MCC) prior to hour 6 of the forecast which propagated eastward and gave widespread generally light rainfall (<1 cm) to eastern Pennsylvania and southeastern New York by hour 12. Although every integration predicted rainfall associated with the MCC, which was present at the initial time, none predicted rain from the squall line, which formed after the initial

TABLE 1. List of experiments.

Number	Form of convection	Saturation criterion (%)	Rainwater evaporation	Cloud phase	Water loading
1	implicit	100	Yes	—	—
2	explicit	100	No	No	No
3	explicit	100	Yes	No	No
4	explicit	100	No	Yes	Yes
5	explicit	100	No	Yes	No
6	explicit	95	No	No	No
7	explicit	95	Yes	Yes	Yes
8	explicit	90	Yes	Yes	Yes

TABLE 2. Observed and predicted total rain volume, maximum rainfall at a single point, and phase error of the rainfall maximum. Observed values are taken from Bosart and Sanders (1981).

Experiment number	Rain volume (10^{12} kg)	Maximum rainfall (cm)	Phase error (km)
Observed	2.15	10.5 [6]*	—
1	3.31	6.4 [6.1]**	119 (SSE)
2	2.69	20.8	296 (E)
3	0.04	0.3	83 (E)
4	0.04	0.4	83 (E)
5	2.59	19.2	296 (E)
6	4.22	20.4	166 (E)
7	1.79	10.6	125 (E)
8	2.84	28.7	83 (E)

* Value in parentheses is the area-averaged maximum observed rainfall on the ½° latitude–longitude grid.

** Value in parentheses is the rainfall maximum closest in location to the observed maximum.

time. This failure may relate to limitations in initial data or model resolution, or to a common factor missing from both the explicit and implicit convection formulations.

Experiment 2 repeated the previous integration, but without cumulus parameterization, using instead the simplest form of explicit heating, whereby water vapor was predicted and no evaporation or rain-water loading was included. Figure 2 shows that the pattern of forecast precipitation sharply differed; the maximum value exceeded 20 cm, more than three times the observed, and was almost 300 km east of its observed location. More than 15 cm fell in a region of central Pennsylvania where less than 2 cm was observed.

Examination of hourly rainfall rates in Experiment 2 showed that the vast majority of rain fell after hour 6, whereas in nature significant rain occurred much earlier (Bosart and Sanders, 1981). In addition, excessive localized rainfall rates of nearly 200 cm d^{-1} occurred, which resemble the explicit heating instabilities seen by other investigators, as described earlier.

This local overprediction of precipitation by the explicit approach was viewed by examining hourly variations of rainfall, equivalent potential temperature (θ_e), saturated equivalent potential temperature (θ_{es}), and vertical motion (ω). Figure 3 compares θ_e and θ_{es} profiles for the implicit and explicit approaches at a point where the explicit approach produced excessive rain. In the parameterized integration at hour 6 (left panel), precipitation had already occurred and ended. The sounding showed a nearly constant θ_e in the lower troposphere and a low-level stable layer produced by two processes: parameterized downdraft cooling and reduction of diurnal warming by clouds. This behavior is similar to that described in 1° latitude–longitude integrations discussed by MC.

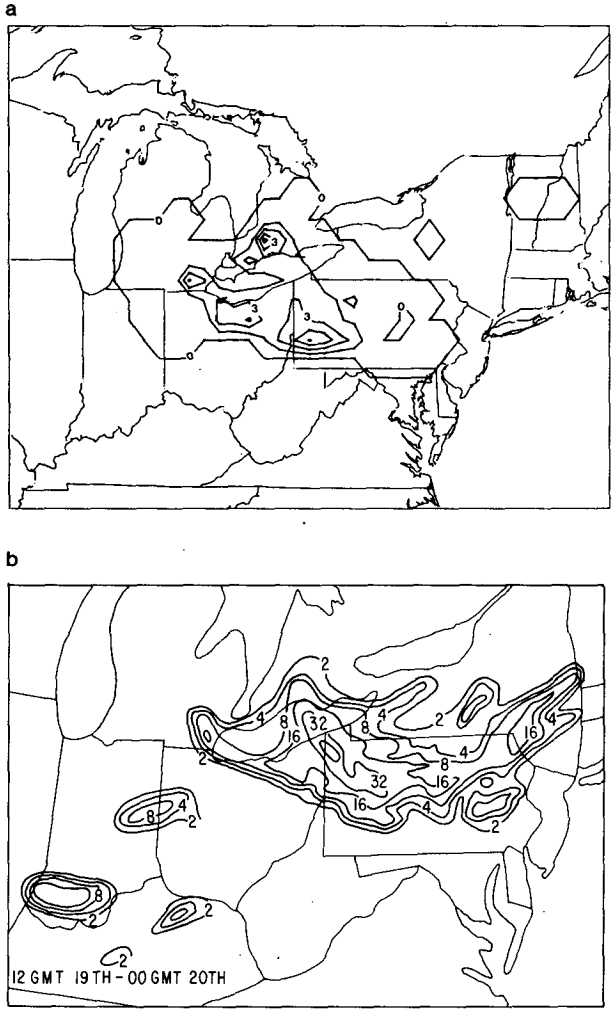

FIG. 1. Rainfall from 1200 GMT 19 July to 0000 GMT 20 July 1977: (a) Predicted (cm) for Experiment 1 with parameterized convective heating (interval: 1.5 cm) and (b) observed (mm) (from Bosart and Sanders, 1981). Contours increase from 2 mm in powers of two.

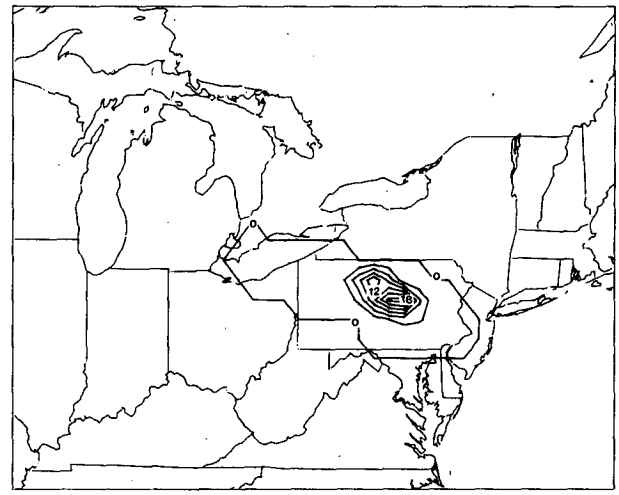

FIG. 2. As in Fig. 1a but for Experiment 2 with explicit heating and no evaporation or cloud water (interval: 3 cm).

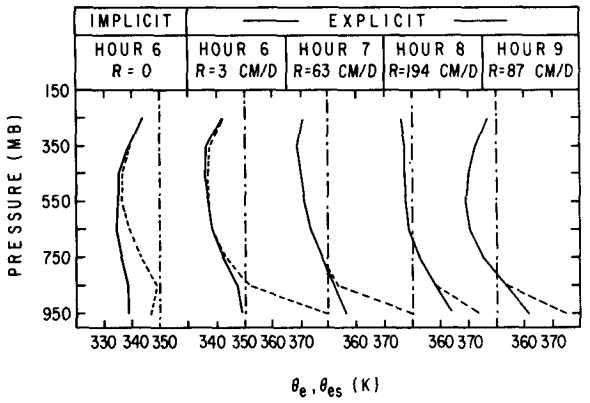

FIG. 3. Left panel: θ_e (solid) and θ_{es} (dashed) for a grid point in the parameterized heating integration at hour 6. Right four panels: Evolution of θ_e and θ_{es} at the same grid point for the simplest explicit formulation (Experiment 2), from hours 6–9 during the explicit heating instability. Instantaneous rainfall rates at each hour are given above the curves. The dashed–dotted vertical lines are drawn at θ_e = 350 K at each hour.

The right four panels in Fig. 3 show the fundamentally different evolution in the explicit heating integration. Rainfall was delayed in Experiment 2 by the requirement of saturation, which did not occur at the given point until just prior to hour 6 (1400 LST). As a result, the diurnal cycle continued unabated until then and strong low-level instability was generated. At the same time, grid-scale forcing was producing upward motion and associated moistening and destabilization aloft. The result by hour 6 was a nearly saturated, highly unstable column which is rarely, if ever, observed on this scale in nature. Once saturation occurred (initially at 650 mb), a feedback growth initiated between vertical motion and heating in the unstable column. In this simplest explicit approach, no evaporation or vertical eddy fluxes were present to stabilize the column, and vertical circulation continued to intensify (see Fig. 4).

In nature, eddy fluxes act to stabilize in two ways: updrafts remove high-energy air from low levels and deposit it aloft with little mixing between, and downdrafts replace this air with lower θ_e air from midlevels. In the explicit formulation, the low-level, high-θ_e air can reach upper levels only by explicit advection on the grid; as a result, high θ_e air must pass through middle levels. The result in the growing circulation by hour 8 was that θ_e and θ_{es} decreased with height through the entire model troposphere; this enhanced the feedback instability, and rainfall rates reached 200 cm d^{-1}. Figure 4 shows that the level of maximum vertical motion shifted upward with time, and subsequent midlevel "entrainment" from adjacent grid points eventually stabilized the column somewhat by hour 9, but the observed 12-h rainfall at the grid point had already been greatly exceeded.

In an attempt to control this instability, additional physical processes were added. Experiment 3 incorporated the evaporation of rainwater. The low-level stabilization produced by this process, which was enhanced by relatively dry low-level air over eastern and central Pennsylvania, not only prevented instability but produced little rainfall (Table 2). Experiment 4, with a cloud-water phase and hydrostatic water loading, but no rain-water evaporation, also produced almost no precipitation. In Experiment 5, the cloud-water equation was kept, but water loading was eliminated. In this experiment, nearly as much rain occurred as in Experiment 2 with no cloud phase.

The reasons for the striking differences between the explicit heating experiments were investigated (Fig. 5) by examining hourly precipitation rates averaged over the grid. In Fig. 5, even the largest rainfall rate shown represents less than 0.01 cm d^{-1} averaged over the grid. The parameterized integration had 100 times the rainfall of the experiments shown at hour 1, and by hour 9 the simplest explicit approach produced 100 times its rainfall at hour 5. Thus the first 7 hours of all explicit integrations produced very little rainfall, despite the rapidly growing curves shown in Fig. 5.

The addition of the cloud phase without water loading differs from the simplest explicit formulation only in that precipitation is delayed until 0.5 g kg^{-1} of cloud water accumulates, but heat is released at the same time in both experiments, and the cloud water is a passive constituent once it forms. Thus the predicted rainfall in Experiments 2 and 5 was quite similar, differing on the order of the total stored liquid water (an

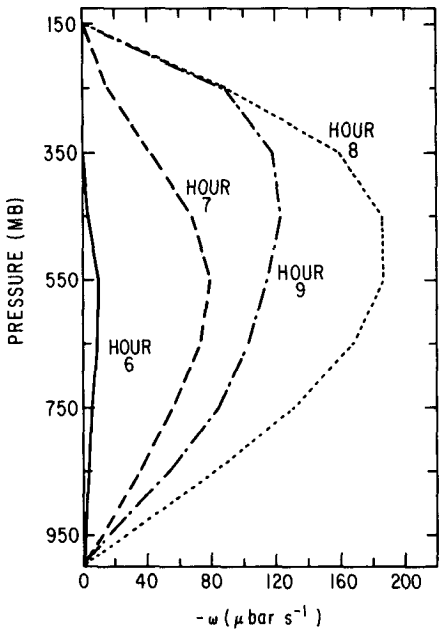

FIG. 4. Evolution of vertical velocity ω (μb s^{-1}) during the explicit heating instability at the point shown in Fig. 4.

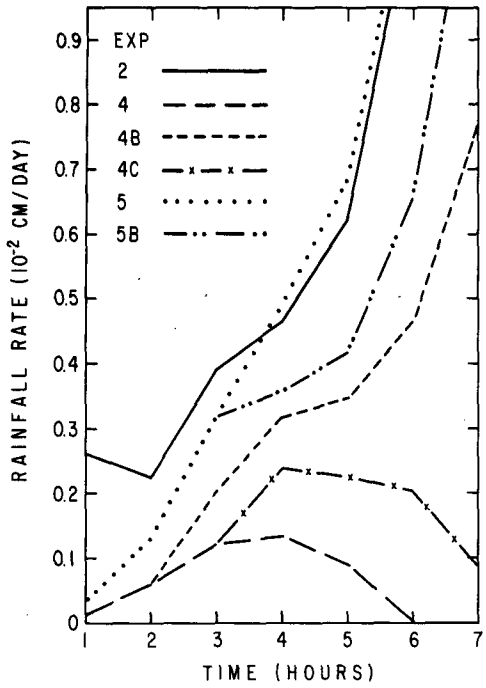

FIG. 5. Time series of instantaneous precipitation rate averaged over the grid for various explicit experiments (10^{-2} cm d^{-1}). Experiment 2 used the simplest explicit approach; Experiment 4 added a cloud-water phase with water loading; and Experiment 5 included the cloud phase but without water loading. Experiments 4b and 4c abruptly removed water loading from Experiment 4 at hours 2 and 3, respectively. Experiment 5b added water loading to Experiment 5 at hour 3.

entire column filled with cloud water in the model at 0.5 g kg^{-1} represents about 0.35 cm of rain). Figure 5 shows that after an early period when cloud water was being stored, the integrations evolved similarly.

An unexpected result was that the addition of hydrostatic cloud-water loading (Experiment 4) reduced the maximum precipitation from 20.8 to 0.4 cm. Figure 5 shows that when water loading was added, Experiments 4 and 5 steadily diverged. It appears that the integrated effect of water loading, combined with the delay in significant precipitation, suppressed the development of the MCC in the initial state to the degree that subsequent explosive growth was no longer possible. Because most of the explicit rain fell during such brief intense rainfall events, the total rainfall in Experiment 4 was underestimated.

Three additional numerical experiments were carried out to support this hypothesis. In Experiment 5b, water loading was abruptly introduced into Experiment 5 at hour 3. Its effect (Fig. 5) was significant, but it did not prevent the rapid growth of precipitation, only delayed it. In Experiments 4b and 4c, water loading was removed from Experiment 4 at hours 2 and 3, respectively. In the former, the suppressed precipitation rate at hour 2 recovered and precipitation was rapidly growing by hour 7. Starting from hour 3, however, the removal of water loading produced only slow precipitation growth, then a decay to zero as in Experiment 4. The results qualitatively support the conclusion that the integrated influence of water loading over several hours on the evolution of the system prevented sufficient growth to allow for instability later, although the exact nature of this nonlinear process is difficult to untangle.

Experiments 2–5 all used a 100 percent saturation criterion. Because rainfall occurred in nature in the absence of area-averaged saturation, this produced significant delay in the onset of precipitation. The result was either that (i) rainfall was greatly underestimated (Experiments 3 and 4) or (ii) unrealistically large instability developed and, in the absence of the inhibiting effects of water loading and rain-water evaporation, was followed by intense localized rainfall as the instability was released (Experiments 2 and 5).

One potential solution to the lack of meso-α scale saturation prior to rainfall in nature is simply to reduce the saturation criterion (e.g., Orlanski and Ross, 1984). By the earlier definitions, this does not blur the distinction between implicit and explicit. Rather, the reduced saturation experiments remain explicit because clouds and rain do not occur until saturation is reached, and grid scale values still directly represent the cloud; only saturation itself is redefined.

Experiment 6 was identical to Experiment 2, except a 95 percent saturation criterion was adopted. Because saturation occurred sooner, the predicted rain area (Fig. 6) extended further upstream than in Experiment 2. However, unstable growth of precipitation also occurred sooner and over a wider area, and precipitation volume (Table 2) was greatly overestimated. When both rain evaporation and water loading were added

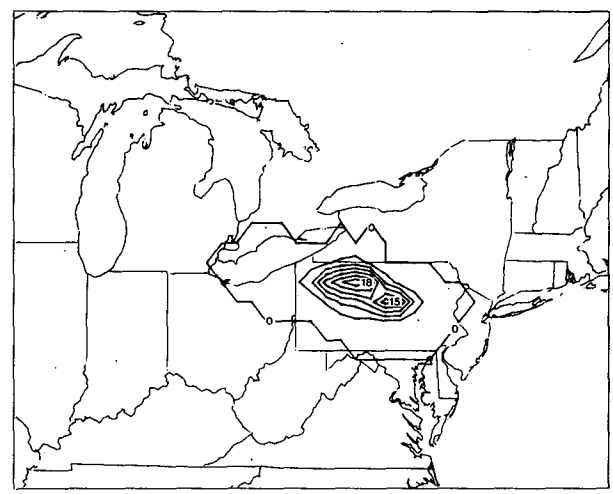

FIG. 6. As in Fig. 1a but for Experiment 6, which used a 95 percent saturation criterion and no cloud phase or rain-water evaporation.

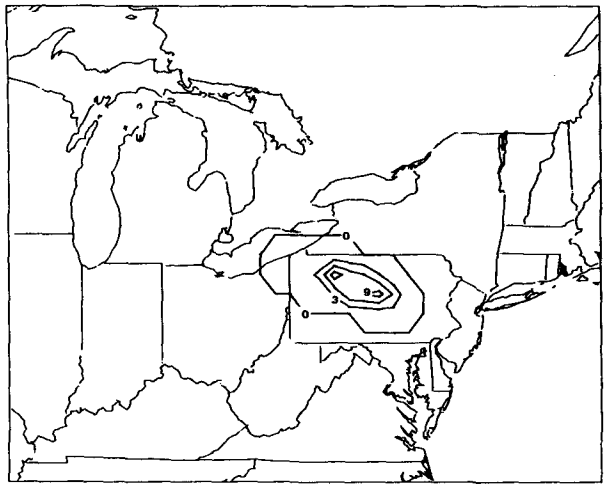

FIG. 7. As in Fig. 1a but for Experiment 7, which used a 95 percent saturation criterion with a cloud phase and rain-water evaporation.

(Experiment 7), the best explicit precipitation forecast was obtained (Fig. 7). The saturation delay was still present and led to the rainfall maximum being too far downstream and the rain volume being underestimated. Nevertheless, the magnitude of error was comparable to that of the implicit heating integration.

In an effort to reduce the phase error further, Experiment 8 used a 90 percent saturation criterion and was otherwise identical to the previous experiment. Although this integration produced the smallest phase error, the instability problem returned. The cause was the same as previously: a deep layer of convective instability formed after hour 8, and 19 cm of rain fell in the last four hours at a single grid point. This experiment showed that the inclusion of effects that inhibit updraft growth does not necessarily remove the instability problem in meso-α scale models.

6. Discussion

a. *Explicit instabilities*

The use of explicit heating imposes two requirements: (i) that saturation be reached on the grid scale prior to any condensation or precipitation and (ii) that subgrid-scale eddy fluxes can be neglected. The combined influence of these constraints acted to encourage localized instabilities in the simplest explicit formulation. The saturation requirement delayed the onset of precipitation well beyond when it was observed in nature. During this period, upward motion destabilized the column, and diurnal warming, unreduced by clouds or rain, caused large low-level destabilization. Saturation ultimately occurred in the regions of upward motion, but it was accompanied by such a strongly unstable sounding that heating and vertical motion grew rapidly. Due to the lack of eddy fluxes, unrealistic θ_e and θ_{es} profiles evolved, for which high low-level values were advected to midlevels, eventually producing convective instability through the entire model troposphere. A violent overturning followed, with unreasonably large rainfall rates given the 2500 km^2 grid area.

The addition of simple forms of rainwater evaporation and a cloud phase with hydrostatic water loading eliminated the instability when a 100 percent saturation criterion was used. Because the explicit instability found by others (Koch et al., 1985; Zack et al., 1985; Dare et al., 1985) also occurred using the simplest form of explicit heating, these results suggest that such instabilities could be controlled by the inclusion of inhibiting effects on updraft growth. Nevertheless, the nature of the instability in this study appears to differ from those of previous authors, all of whom reported large heating at low levels. In the current study, heating was small at low levels during the blowups, and the level of maximum heating rose from the middle to upper troposphere as the instability occurred (see ω field evolution in Fig. 4). The instability arose not due to excessive heating at low levels, but as a result of the unrealistic stability evolution brought about by the requirements of explicit heating.

When the saturation criterion r_{sat} was reduced to 0.95 and full inhibiting effects were included, predicted rainfall was comparable in accuracy to the parameterized integration. When $r_{sat} = 0.9$ was used, however, excessive localized rainfall once again occurred. Although the dependence of rainfall on the saturation criterion is case-dependent, the latter result shows that even when water loading and rain-water evaporation are present, instability may occur with the explicit approach. The presence of diurnal warming was an essential contributor to the conditions that led to unstable growth of rainfall. The lack of instability in the study of Hsie and Anthes (1984), even with the simplest explicit heating, may reflect the lack of a diurnal cycle in their simulations.

b. *Roles of additional microphysics and higher resolution*

This work compared a developed cumulus parameterization with very simple explicit approaches and thus is potentially biased toward the implicit approach. In particular, a rainwater prediction equation (Type III) was not included. Two difficulties may reduce the value of a Type III approach.

(i) The saturation delay problem exists to the same extent regardless of microphysics, which enters only once saturation has occurred. Where this delay is a problem, such as in the 100 percent saturation criterion experiments, additional microphysics would likely contribute little.

(ii) On the meso-α scale, updraft (or downdraft)

strength cannot approach its true value in cumulonimbus clouds in nature. The role of raindrop terminal velocity and such processes as accretion of cloud droplets by rain are distorted by unrepresentative updraft strength on the meso-α scale grid (e.g., drops would fall too rapidly in weak updrafts). When the formulations for such processes are taken directly from nonhydrostatic cloud models, the errors introduced could be of the same order as the benefits.

For these reasons, it does not appear that the inclusion of more sophisticated microphysics would substantially improve the performance of the explicit approach in meso-α scale models. Because implicit approaches are more amenable to improvement, and the best explicit integration was only comparable in performance, implicit approaches may have the greatest potential for success when the grid spacing exceeds 50 km.

On the meso-β scale, however, the issues are not so clear. For example, the saturation delay problem was reduced considerably by the increase in resolution from 1° to ½° (compare rainfall predicted by the simplest explicit formulation in this study and MC), and more improvement would be expected with a further increase in resolution to the meso-β scale. The second problem would also become less significant with decreasing grid size, as updraft/downdraft strength approached closer to values observed in clouds in nature.

Recently, Zhang (1985) used a meso-β scale model to forecast the same case as in this study from the same initial time, with a similar initial state. Using the simplest explicit approach, Zhang found excessive localized precipitation, much like in this study, but further west because the start of precipitation was not delayed with his 25 km grid spacing. Because the delay problem was not a factor on this scale, the inclusion of more sophisticated microphysics would be likely to improve the simulation. Nevertheless, Zhang found that an implicit approach (following Fritsch and Chappell, 1980) produced an excellent forecast of the system, including the squall line to the east of the MCC. A key factor in this success was the simultaneous presence of updrafts and (parameterized) downdrafts at a grid point, which is part of the parameterization used in the current study but cannot be simulated with an explicit approach, regardless of its microphysical parameterization. The issue of implicit versus explicit treatment of cumulus convection remains unresolved on the meso-β scale.

c. *Conclusions*

The mesoscale convective complex in this study existed with relatively weak grid-scale forcing, and the evolution of the system was controlled by the sources and sinks of latent heating, as noted by MC. The relative performance of implicit and explicit approaches might be quite different for a well-developed disturbance with strong grid-scale forcing. Nevertheless, the following conclusions appear to be of widespread validity for meso-α scale models.

(i) The simplest form of explicit heating, whereby condensed water falls immediately as rain with no additional physics, was highly prone to instability. Because such instability has been encountered by several researchers under various dynamic and thermodynamic conditions, the simplest explicit approach appears to be inappropriate for mesoscale (or any scale) models in convectively unstable regions.

(ii) The frequent instability problems of the explicit approach were significantly reduced by the addition of rainwater evaporation and a cloud-water phase with hydrostatic-water loading.

(iii) Because rain occurred in nature in the absence of meso-α scale saturation, precipitation was delayed in the explicit approach and serious errors in predicted stability and rainfall resulted, especially in the integrations with a 100 percent saturation criterion.

(iv) Reducing the saturation criterion in order to reduce the delay problem produced improved phase errors in the rainfall prediction, but a systematic error remained and local instabilities sometimes reappeared. Although the best explicit forecast, using a formulation similar to that of Orlanski and Ross (1984), had errors comparable to the implicit integration, the greatest possibility for improvement in meso-α scale models appears to lie with implicit approaches.

On the meso-β scale, the choice between implicit and explicit cumulus convection remains unresolved, but the potential benefits of more sophisticated microphysics are greater, and the fundamental advantage of not having to specify the convective scale–large scale interactions a priori makes the explicit approach potentially of value. It is unclear at what scale the explicit formulation consistently outperforms implicit approaches in hydrostatic models. Further numerical experiments will be undertaken to address this question for both meso-α and meso-β resolution, for disturbances which differ from the current study in moisture content and strength of grid scale forcing, and will be reported on at a later time.

Acknowledgments. This research is supported by National Science Foundation Grant ATM-8317104.

REFERENCES

Anthes, R. A., Y.-H. Kuo and J. R. Gyakum, 1983: Numerical simulations of a case of explosive marine cyclogenesis. *Mon. Wea. Rev.*, **111**, 1174–1188.

Bosart, L. F., and F. Sanders, 1981: A long-lived convective system. *J. Atmos. Sci.*, **38**, 1616–1642.

Dare, P. M., P. J. Smith and J. T. Shively, 1985: The role of convective and stable latent heat release in the development of an extratropical cyclone. *Preprints Seventh Conf. on Numerical Weather Prediction*, Montreal, Amer. Meteor. Soc., 232–236.

Frank, W. M., 1983: The cumulus parameterization problem. *Mon. Wea. Rev.*, **111**, 1859–1871.

——, and C. Cohen, 1985: Properties of tropical cloud ensembles estimated using a cloud model and an observed updraft population. *J. Atmos. Sci.*, **42,** 1911–1928.

Fritsch, J. M., and C. F. Chappell, 1980: Numerical prediction of convectively driven mesoscale pressure systems. Part II: Mesoscale model. *J. Atmos. Sci.*, **37,** 1734–1762.

Grammeltvedt, A., 1969: A survey of finite difference schemes for the primitive equations for a barotropic fluid. *Mon. Wea. Rev.*, **97,** 384–404.

Hsie, E., and R. A. Anthes, 1984: Simulations of frontogenesis in a moist atmosphere using alternative parameterizations of condensation and precipitation. *J. Atmos. Sci.*, **41,** 2701–2716.

——, —— and D. Keyser, 1984: Numerical simulation of frontogenesis in a moist atmosphere. *J. Atmos. Sci.*, **41,** 2581–2594.

Johnson, R. H., 1976: The role of convective scale precipitation downdrafts in cumulus and synoptic scale interactions. *J. Atmos. Sci.*, **33,** 1890–1910.

Kanamitsu, M., 1975: On numerical prediction over a global tropical belt. Ph.D. thesis, Florida State University, 281 pp.

Kasahara, A., 1961: A numerical experiment on the development of a tropical cyclone. *J. Meteor.*, **18,** 259–282.

Koch, S. E., W. C. Skillman, P. J. Kocin, P. J. Wetzel, K. F. Brill, D. A. Keyser and M. C. McCumber, 1985: Synoptic scale forecast skill and systematic errors in the MASS 2.0 model. *Mon. Wea. Rev.*, **113,** 1714–1737.

Kreitzberg, C. W., and D. J. Perkey, 1976: Release of potential instability: Part I. A sequential plume model within a hydrostatic primitive equation model. *J. Atmos. Sci.*, **33,** 456–475.

Krishnamurti, T. N., M. Kanamitsu, R. Godbole, C. B. Chang, F. Carr and J. Chow, 1976: Study of a monsoon depression (II), dynamical structure. *J. Meteor. Soc. Japan,* **54,** 208–225.

Kuo, H. L., 1974: Further studies of the parameterization of the influence of cumulus convection on large scale flow. *J. Atmos. Sci.*, **31,** 1232–1240.

Leary, C. A., and R. A. Houze, 1980: The contribution of mesoscale motions to the mass and heat fluxes of an intense tropical convective system. *J. Atmos. Sci.*, **37,** 784–796.

Lilly, D. K., 1960: On the theory of disturbances in a conditionally unstable atmosphere. *Mon. Wea. Rev.*, **88,** 1–17.

Lord, S. J., H. E. Willoughby and J. M. Piotrowicz, 1984: Role of a parameterized ice-phase microphysics in an axisymmetric, nonhydrostatic tropical cyclone model. *J. Atmos. Sci.*, **41,** 2836–2848.

Molinari, J., 1985: A general form of Kuo's cumulus parameterization. *Mon. Wea. Rev.*, **113,** 1411–1416.

——, and T. Corsetti, 1985: Incorporation of cloud-scale and mesoscale downdrafts into a cumulus parameterization: Results of one- and three-dimensional integrations. *Mon. Wea. Rev.*, **113,** 485–501.

Ooyama, K. V., 1982: Conceptual evolution of the theory and modeling of the tropical cyclone. *J. Meteor. Soc. Japan,* **60,** 369–379.

Orlanski, I., and B. B. Ross, 1984: The evolution of an observed cold front. Part II: Mesoscale dynamics. *J. Atmos. Sci.*, **41,** 1669–1703.

Phillips, N. A., 1979: The nested grid model. NOAA Tech. Rep. NWS22, 80 pp. [Available from Environmental Science Information Center (D822), NOAA, Rockville, MD 20852.]

Rosenthal, S. L., 1978: Numerical simulation of tropical cyclone development with latent heat release by the resolvable scales. I: Model description and preliminary results. *J. Atmos. Sci.*, **35,** 258–271.

——, 1979: The sensitivity of simulated hurricane development to cumulus parameterization details. *Mon. Wea. Rev.*, **107,** 193–197.

Ross, B. B., and I. Orlanski, 1978: The circulation associated with a cold front. Part II: Moist case. *J. Atmos. Sci.*, **35,** 445–465.

——, and ——, 1982: The evolution of an observed cold front. Part I. Numerical simulation. *J. Atmos. Sci.*, **39,** 296–327.

Takeda, T., 1965: The downdraft in convective shower-cloud under the vertical wind shear and its significance for the maintenance of convective system. *J. Meteor. Soc. Japan,* **43,** 302–309.

Yanai, M., S. Esbensen and J. Chu, 1973: Determination of bulk properties of tropical cloud clusters from large-scale heat and moisture budgets. *J. Atmos. Sci.*, **30,** 611–627.

Zack, J. W., M. L. Kaplan and V. C. Wong, 1985: A comparison of the prognostic performance of several cumulus parameterizations in mesoscale simulations of the 10 April 1979 SESAME I case. *Preprints Seventh Conf. on Numerical Weather Prediction,* Montreal, Amer. Meteor. Soc., 415–422.

Zhang, D.-L., 1985: Nested-grid simulation of the meso-β scale structure and evolution of the Johnstown flood of July 1977. Ph.D. dissertation, Pennsylvania State University, 270 pp.

Zipser, E. J., 1980: Kinematic and thermodynamic structure of mesoscale systems in GATE. *Proc. Seminar on the Impact of GATE on Large-Scale Numerical Modeling of the Atmosphere and Ocean,* Woods Hole, MA., National Academy of Sciences, 91–99. [Available from the U.S. Committee for the Global Atmospheric Research Program, 2101 Constitution Ave., Washington, D.C., 20418.]